STUDY ON THE EFFECTIVENESS OF THE HIGH DUCTILITY ASEISMATIC JOINT SPLICED PILES SUBJECTED TO LIQUEFACTION-INDUCED LARGE GROUND DISPLACEMENTS

T.MIYASAKA[1], Y.ITOU[2], H.KASAHARA[3], T.MATUMOTO[4], Y.MATSUKI[5], K.TAKANO[6] and D.HIRATA[7]

1,2 : Daido Concrete Co., Ltd., 2-10-14 Ryougoku Sumida-Ku, Tokyo
3 : Maeda Concrete Industry Ltd., 3-23-21 Touyou Koutou-Ku, Tokyo
4 : Sintoku Kogyo Co., Ltd., 32-7-303 Aoi 3-Chome Adachi-Ku, Tokyo
5 : Nippon High Strength Concrete Co. Ltd., 1-4-9 Nishishinbashi Minato-Ku, Tokyo
6 : Jiban Sikenjyo Corporation, 4-29-5 Midori, Sumida-Ku Tokyo
7 : Yamaguchi University, 2557 Tokiwadai, Ube City, Yamaguchi Prefecture

ABSTRACT

In order to minimize the damages of structures resulted by earthquake, a energy dissipating device is necessary. In this paper, a newly developed High Ductility Aseismatic Joint(H.D.A.J.) was introduced. In order to elucidate the bending characteristics of H.D.A.J. spliced pile, authors performed a series of bending experiments. Meanwhile, a nonlinear FEM which considered both geometric and material nonlinearities of pile and material nonlinearity of soil, was proposed. By simulating the experiment results, the validity of the method was checked. Then the method was applied to examine the effectiveness of H.D.A.J. spliced piles subjected to liquefaction-induced large ground displacements. Based on the numerical analyses, the parametric study was performed. Consequently, in all cases, the effectiveness of H.D.A.J. spliced piles subjected to liquefaction-induced large ground displacements are verified.

KEYWORDS

pile foundation; energy dissipating device; aseismatic joint; high ductility; spliced pile; liquefaction; lateral ground displacement.

INTRODUCTION

There are several different types of ground motion caused by earthquake. Particularly, the ground motion caused by soil liquefaction is a typical phenomenon. In accordance with the aviation pictures that sometimes this ground motion results a large permanent displacement up to several meters. Due to the large ground displacement, not only the superstructures but also the substructures such as buried pipes and pile foundation were destroyed. So far, the effect of large ground displacements on underground structures has been studied. In the mean time, Stewart et al. (1988) and Miura et al. (1989,1990) proposed a nonlinear finite element method to analyze the performance of piles subjected to liquefaction-induced large ground displacements. The geometric and material nonlinearities of the pile and the material nonlinearity of the soil were taken into consideration.

In spite of the remarkable improvement of concrete material, the recent post-earthquake investigation reports revealed that the concrete foundation piles were seriously damaged during the earthquake. Authors examined the performance of the prestressed high strength concrete piles when subjected to large ground displacements and found that the piles would develop a plastic hinge at the interface between the liquefied layer and nonliquefied layer when the lateral displacement of the ground reached 10 to 20 cms(Miyasaka et al. 1994). Some experts have pointed out that the main reason of such damages may possibly be caused by the shortage of ductility of pile itself and that the most effective and economical measures is the use of the energy dissipating device. Based on this view point, authors newly developed a High Ductility Aseismatic Joint(H.D.A.J.) and applied it to foundation pile to create a high energy absorption pile foundation structure

which prevent the ultimate destruction caused by earthquake.

In this study, we first explain the basic and mechanism of H.D.A.J.. Second, two types of H.D.A.J. which have different thickness of attenuation rubber were mounted in two different diameter precast prestressed concrete piles. The bending characteristics of these spliced piles were elucidated by experiments. All information obtained from the experiments were used for analysis. The validity of nonlinear FEM was checked by simulating the experiment result. Finally, authors conducted a series of parametric study on the affect of splicer type, stratum thickness, magnitude of axial load, cap rigidity, pile tip embedded length et al. to investigate the effectiveness of H.D.A.J. spliced pile subjected to liquefaction-induced permanent ground displacements.

BASIC AND MECHANISM OF HIGH DUCTILITY ASEISMATIC JOINT

The crossed section and the basic structure of H.D.A.J. are shown respectively in figure 1 and figure 2. In this joint structure, three main components are provided : the pile tip fittings with circumferential groove, a circumferentially multi-devided cylindrical inner ring with projections on which the attenuation rubbers are attached, and an integral cylindrical outer ring. The splicing procedure is first setting the upper pile vertically onto the lower pile, then engaging the projections of inner rings with the groove of pile tip fittings, and finally pushing the outer ring in the longitudinal direction of piles to fasten the inner ring by the effect of inverse conical taper in the fitted surface of the inner ring and the outer ring. The splicing is conducted by hydraulic jacks and controlled by pushing pressure. In this study, two kinds of joint are used, X type, and Y type. The only one difference of these two types of joint is the thickness of attenuation rubber, 2 mm thick for X type joint, and 4 mm thick for Y type joint.

BENDING CHARACTERISTICS EXPERIMENTS

A series of bending characteristics experiments were performed. The schematical diagram of the specimen is shown in figure 3. The span length is 7.2 m. The Rotational angle - θ, surface strain - ε and deflection - δ were measured as shown in figure. Table 1 summarizes the experiment cases. All tested piles were B type prestressed high strength concrete piles which have a prestress of 80 kgf/cm^2.

Two examples of the relationships of bending moment to the rotational angle obtained from experiment s are shown in figure 4(a) and (b). A brief test results of all experiments are shown in Table 2. The bending moment defined here is the sum of the bending moment caused by self weight of pile, effect of axial load, and the applied test load. The rotational angle defined here is the value of unit length of 0.5 m, is converted from the experiment results. Figure 4(a), and (b) shows the results of the case 1 to 3, and the case 7 to 9 respectively, i.e. the cases without axial load. In case of 400mm dia. pile, the pile with X type joint, and the pile with Y type joint has the ultimate rotational angle of 2.6 times, and 4.7 times that of the pile without joint respectively. In case with an axial load of 60 tf, the ratios become 3.5, and 6.1 respectively. In case of 600mm dia. pile, the pile with X type joint, and the pile with Y type joint has the ultimate rotational angle of 2.6 times, and 4.4 times that of the pile without joint respectively. In case with an axial load of 130 tf, the ratios become 3.1, and 6.7 respectively. In other words, the use of H.D.A.J. provides piles with higher ductility.

NUMERICAL ANALYSIS METHOD

Figure 5 illustrates the model for numerical analyses. In order to express the geometric and material nonlinearity of the pile, a pile is model by arranging beam element and rotational spring slider element one after the other. The stiffness matrix of the beam element is given as;

$$\begin{bmatrix} \frac{EA}{l} & 0 & 0 & -\frac{EA}{l} & 0 & 0 \\ & \frac{12EI}{l^3}+\frac{6P}{5l} & \frac{6EI}{l^2}+\frac{P}{10} & 0 & -\left(\frac{12EI}{l^3}+\frac{6P}{5l}\right) & \frac{6EI}{l^2}+\frac{P}{10} \\ & & \frac{4EI}{l}+\frac{2PL}{15} & 0 & -\left(\frac{6EI}{l^2}+\frac{P}{10}\right) & \frac{2EI}{l}-\frac{Pl}{30} \\ & & & \frac{EA}{l} & 0 & 0 \\ & \text{symm.} & & & \frac{12EI}{l^3}+\frac{6P}{5l} & -\left(\frac{6EI}{l^2}+\frac{P}{10}\right) \\ & & & & & \frac{4EI}{l}+\frac{2PL}{15} \end{bmatrix} \quad (1)$$

In which l is the length of the element, E is Young's modules, A is the area of the section, I is the moment of inertia, and P is the axial load. This stiffness matrix is a function of P, and this makes it possible to express the so called P- Δ effect. When P is equal to zero, this stiffness matrix is equal to the ordinary linear stiffness matrix of small deflection problems.

The coordinates of the nodal points of the beam elements and therefore the stiffness matrix of the elements are updated at each load step. Through the iteration, geometric nonlinearity of the pile is actualized. The material nonlinearity of the pile is expressed by the rotational spring slider element. In this study, the relationships between bending moment and rotational angle obtained from experiments were used for analyses. The values of Young's modules used in the analyses are shown in Table 3. These values were obtained from experimental bending moment vs. rotational angle curve below the cracking level. It should be noted that the values for the cases with axial load are larger than those for the cases with no axial load.

NUMERICAL SIMULATIONS OF EXPERIMENTS

Figure 5(a) and (b) compare the bending moment-deflection curves obtained from the experiments and the numerical simulations. Figure (a), and (b) compares the results from the case 1 to 3, and the case 7 to 9 respectively. The triangle marked lines show the results from the experiments, and the rhombus marked lines show the results from the simulations. These figures show good agreement between the experiments and the simulations in all cases. These conformities verify the validity of the proposed analysis method.

RESPONSE CHARACTERISTICS TO LATERAL GROUND DISPLACEMENTS

Analysis model

Figure 6 illustrates the analysis model for parametric study. The soil stratum of ground is assumed as 3 layers, the surface nonliquefiable layer, the middle liquefiable layer, and the basal nonliquefiable firm layer. The ground lateral displacements distribution is assumed as trapezoid as shown in figure. The pile is modeled by the rotational spring sliders element and beam element arranged one after the other. The pile-soil interaction is modeled by a spring slider element which has a by-linear relationship between the force and the displacement. An extra rotational spring slider element is used at the pile head to adjust the pile cap Connectivity.

Parametric study cases

a)Pile outside diameter: 400mm dia. pile and 600mm dia. pile are used.
b)Joint type: Non-joint, X type, and Y type are used.
c)Surface layer thickness ratio: The upper layer thickness, i.e. the total thickness of the surface layer and the middle layer, is assumed as a constant of 12 m. 4 ratios of surface layer thickness-(h) to the upper layer thickness-(H) are used, h/H=1/2, 1/4, 1/8, and 0
d)Connectivity: 100%(fixed), 50%, and 0%(hinged) are used.
e)Embedded length into basal layer: For 400mm dia. pile, 0.5m and 1.0m, for 600mm dia. pile, 1.0m and 1.5m are used.

Analysis results

a)Affect of surface layer thickness ratio on bending moment distribution

Bending moment distributions along the pile shaft when the first hinge developed, or if no hinge developed but the bending moment kept in stable distribution, are shown in Figure 7 to Figure 10. Figure 7, and Figure 8 shows the analysis results of 400mm dia. pile without joint, and with Y type joint respectively. In the Figure, the broken line indicates the ultimate moment. Viewing over these Figures, the maximum bending moment shows a tendency to concentrate at the boundary of the liquefiabe layer and the nonliquefiable layer independent of the surface layer thickness ratio and the pile cap Connectivity. Except in the case that h/H=0, the lower boundary developed a hinge earlier than the upper boundary in all other cases.
In case that Connectivity is fixed, and h/H=1/2 or h/H=1/4, the bending moment distributed at the pile head is not so large. But when h/H decreases, pile head bending moment increases. When h/H=0, it becomes so large that a hinge develop here earlier than the lower boundary.
In case that Connectivity is 50%, the yield moment is a half of the value of the fixed Connectivity. Both the pile without joint and the pile with Y joints develop first hinge at the lower boundary when h/H is above 1/4, and develop first hinge at pile head when h/H is less than 1/4.
In case that Connectivity is 0%, the bending moment at the upper boundary is quite large when h/H=1/2 or h/H=1/4, and is so small when h/H is less than 1/4. In spite of all other cases develop first hinge at the lower boundary, the pile with Y joints never reach the ultimate moment when h/H is less than 1/4.
Figure 9, and Figure 10 shows the analysis results of 600mm dia. pile without joint, and with Y type joint respectively. The biggest difference compared to 400mm dia. pile is the magnitude of the bending moment at lower boundary. The bending moment distributes at lower boundary is so small that no hinge develops at lower boundary in any case. This phenomenon is based on the small fixation ratio of the pile into the basal stratum, i.e. 1m/0.6m=1.67 in this case.

b)The ground displacement when plastic hinge developed
Comparing the Figure 7(a) and 8(a), the responses of the pile without joint and the pile with Y joints are quite different. In order to evaluate the effects of the jointed piles and the affects of various parameters, the ground displacement when pile developed plastic hinge, hereinafter abbreviated as PHDG displacement, is used as a criterion.
Figure 12, and Figure 13 shows the PHDG displacements of 400mm dia. pile in case that Connectivity is 100%, and 0% respectively. (a) shows the displacement of upper boundary, and (b) shows that of the lower boundary. Viewing over the Figure 12, X joint spliced pile shows a PHDG displacement of 1.5 times, Y joint spliced pile shows 2.0 times that of the pile without joint. Except in the case that h/H=0 of upper boundary, all PHDG displacements decreases when h/H ratio decreases. In case that h/H=0 of upper boundary, bending moment concentrates in pile head and results a different plastic hinge development. First hinge develops at pile head, and second hinge develops at lower boundary. This order is opposite in other cases. The surface layer contributes an effect of dispersion of bending moment near the upper boundary.
Figure 13 shows a similar tendency to Figure 12, except the case that h/H=0 and the case that h/H=1/8 at upper boundary. Both of these two cases have thin surface layer. After the first plastic hinge developed, hinged pile head rotated and released the increase of the bending moment near the upper boundary.

c)Affects of pile diameter
Figure 14(a), and (b) shows the PHDG displacements of 600mm dia. pile in case that Connectivity is 100%, and 0% respectively. Same as the 400mm dia. pile, Y joint spliced pile shows a PHDG displacement of 2 times that of pile without joint. Meanwhile, in case that Connectivity is 100%, the first hinge developed at upper boundary, and the lower boundary never develop plastic hinge. In case that Connectivity is 0%, the upper boundary developed a plastic hinge only when h/H=1/2, the other cases do not develop plastic hinge. This is due to the small fixation of pile tip into the basal stratum, results a hinge-like behavior at the lower boundary.

d)Affects of embedded length into basal layer
As above mentioned, although the embedded length into the basal layer is the same(1m), the developed patterns of plastic hinge are quite different between the case of 400mm dia. pile and the case of 600mm dia. pile. To check the influence of the fixation ratio, we also analyzed the case that embedded length/pile dia. = 1.5m/0.6m = 2.5 for 600mm dia. pile, and the case that 0.5m/0.4m = 1.25 for 400mm dia. pile. We found that plastic hinge developed pattern changed completely depend upon the fixation ratio. Figure 16 shows the affect

of fixation from the view point of upper boundary. Independent of the pile size, the small fixation shows a same response as that when pile developed a plastic hinge at lower boundary.

Evaluation of stability

According to above examination, we found that pile response strongly affected by various parameters, pile dia., joint type, surface nonliquefiabe layer ratio, pile cap Connectivity and fixation ratio. In the mean time, we found that the ultimate situation could be classified into 6 patterns shown in Figure 17.

Pattern A: first hinge at lower boundary, second hinge at upper boundary.
Pattern B: first hinge at pile head, second hinge at upper boundary.
Pattern C: cap Connectivity = 0, first hinge at lower boundary.
Pattern D: first hinge at upper boundary, lower boundary never yield.
Pattern E: first hinge at pile head, lower boundary never yield.
Pattern F: cap Connectivity = 0, lower boundary never yield, surrounding soil yield.

CONCLUSIONS

In this study, a new pile structure, a traditional pile spliced with a high ductility aseismatic joint was developed. The bending characteristics of the new pile structure were elucidated by a series of experiments. Meanwhile, a numerical analysis method was proposed to analyze the pile response subjected to liquefaction-induced large ground displacements. The validity of this method was verified by simulating the results of the experiments. Subsequently, a parametric study was performed to investigate the effect of H.D.A.J. and the affect of pile size, joint type, surface nonliquefiabe layer ratio, pile cap Connectivity and fixation ratio.

Consequently, we found the failures of the pile subjected to the liquefaction-induced large ground displacements could be classified into 6 patterns. In all cases, H.D.A.J. are effective. From the analyses results, we found that the X joint spliced pile could sustain lateral ground displacement of 1.5 times, Y joint spliced pile could sustain lateral ground displacement of 2.0 times that sustained by the pile without joint. However, this study is limited to the response to the permanent ground displacements, the study of the dynamic response of the H.D.A.J. spliced pile is also significant, we would continue the research on this subject.

ACKNOWLEDGMENT

We would like to express our sincere thanks to Professor M.Hamada of Waseda University and Professor F.Miura of Yamaguchi University for the precious information on pile damage caused by post earthquake and the valuable suggestions and instructions on numerical analysis process. Thanks are extended to Professor T.D.O'Rouke and Dr. W.D.Meyersohn for providing information on the newest version of computer code "B-STRUCT".

REFERENCES

1)H.E.Stewart, F.Miura, and T.D.O'Rouke: Pile damage due to large displacement, Proc. of the first Japan-U.S. workshop on liquefaction, large ground deformation and their effects on lifeline facilities, pp.99-126,1988.

2)Hamada,M. and T.D.O'Rourke:Case studies of liquefaction and lifeline performance during past earthquakes, Technical Report NCEER-92-0001, vol.1, and 2, 1992

3)T.Miyasaka, F.Miura, and J.Kiyono: Effects of P- Δ and Connectivity on the nonlinear response of piles subjected to liquefaction-induced large ground displacements, Proc. of the second international conference on earthquake resistant construction and design, Berlin, pp.413-420, 1994.

4)F.Miura, T.Miyasaka, and D.Hirata: High ductility aseismatic joint spliced pile behavior when subjected to liquefaction-induced large ground displacements, Proc. of the 5th U.S. -Japan workshop on earthquake resistant design of pipeline facilities and countermeasures against soil liquefaction, Buffalo, pp.481-494, 1994.

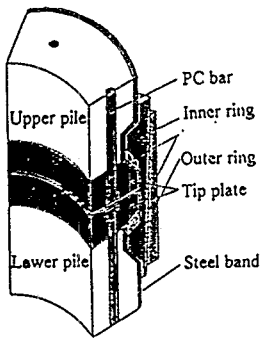

Figure 1 Crossed section of high ductility aseismatic joint

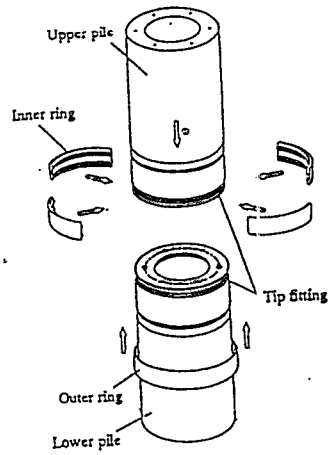

Figure 2 Structure of high ductility aseismatic joint

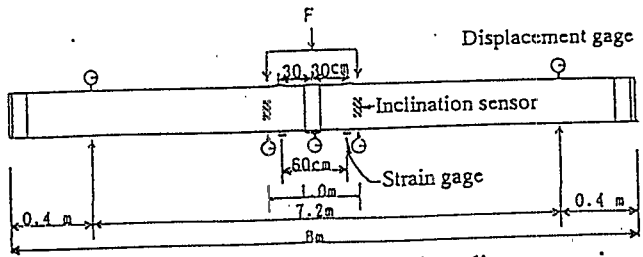

Figure 3 Schematic diagram of bending experiment

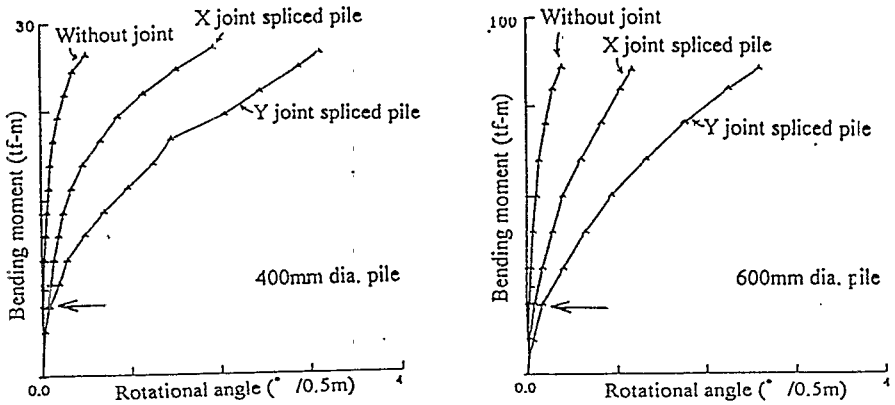

(a) 400mm dia. pile (b) 600mm dia. pile

Figure 4 Experiment results

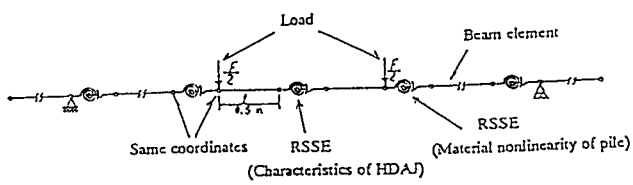

Figure 5 Pile model for numerical simulation

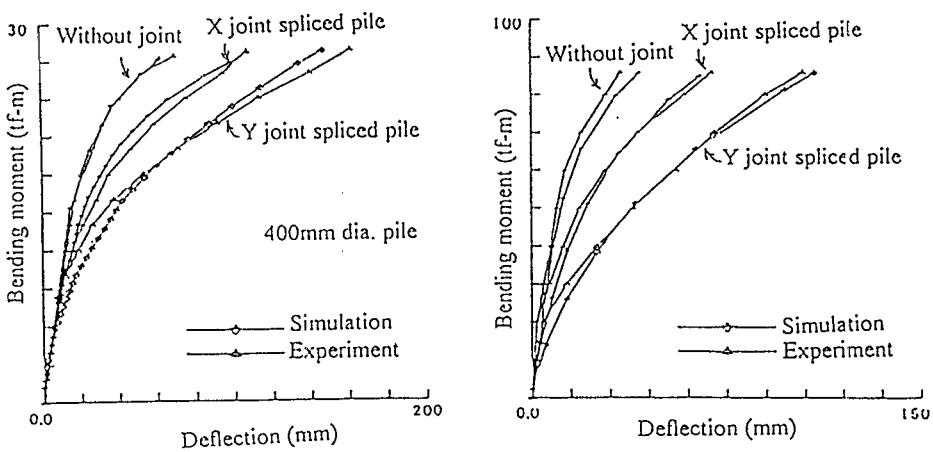

(a) 400mm dia. pile (b) 600mm dia. pile

Figure 6 Simulation of experimental results

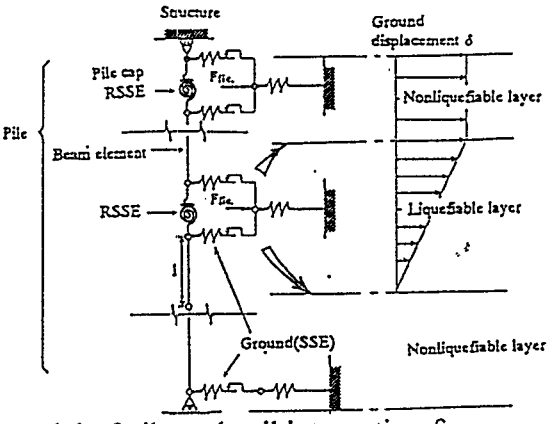

Figure 7 Model of pile and soil interaction for numerical analysis

Table 1 Experiment cases

	Pile diameter (mm)	Span (m)	Axial load (tf)	H.D.A.J. type
Case 1	400	7.2	0.0	Without joint
Case 2	400	7.2	0.0	X joint
Case 3	400	7.2	0.0	Y joint
Case 4	400	7.2	60.0	Without joint
Case 5	400	7.2	60.0	X joint
Case 6	400	7.2	60.0	Y joint
Case 7	600	7.2	0.0	Without joint
Case 8	600	7.2	0.0	X joint
Case 9	600	7.2	0.0	Y joint
Case 10	600	7.2	130.0	Without joint
Case 11	600	7.2	130.0	X joint
Case 12	600	7.2	130.0	Y joint

Table 2 Summary of experiment results

	Ultimate bending moment M_u (tf-m)	Ultimate central deflection y_c (mm)	Ultimate rotational angle θ_u (° /0.5m)
Case 1	19.5	96	0.78
Case 2	19.2	131	2.01
Case 3	19.7	166	3.67
Case 4	27.3	68	0.51
Case 5	27.8	108	1.80
Case 6	26.7	162	3.09
Case 7	61.5	50	0.69
Case 8	60.3	93	1.80
Case 9	60.6	125	3.06
Case 10	86.1	32	0.38
Case 11	85.4	61	1.16
Case 12	85.6	95	2.56

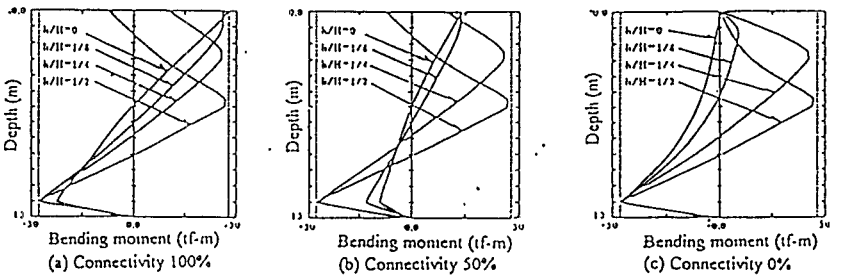

Figure 8 Bending moment distribution : Without joint, 400mm dia. pile

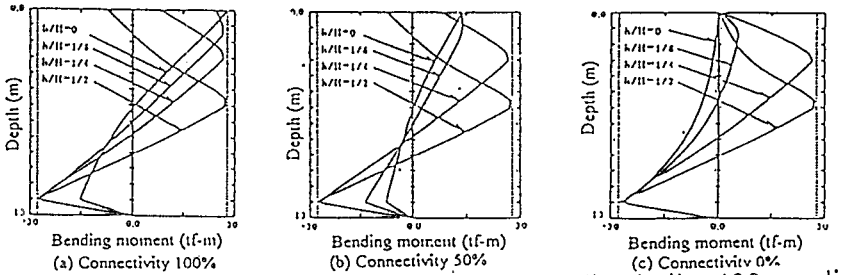

Figure 9 Bending moment distribution : Y joint spliced pile, 400mm dia. pile

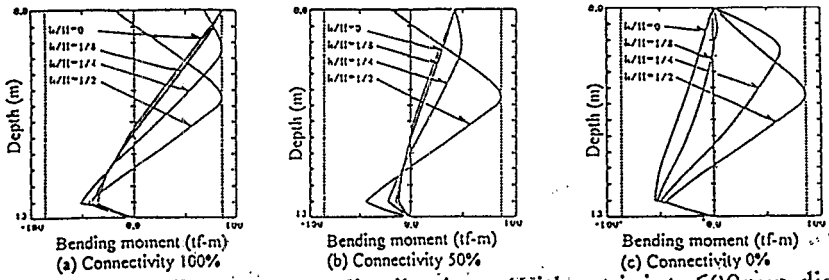

Figure 10 Bending moment distribution : Without joint, 600mm dia. pile

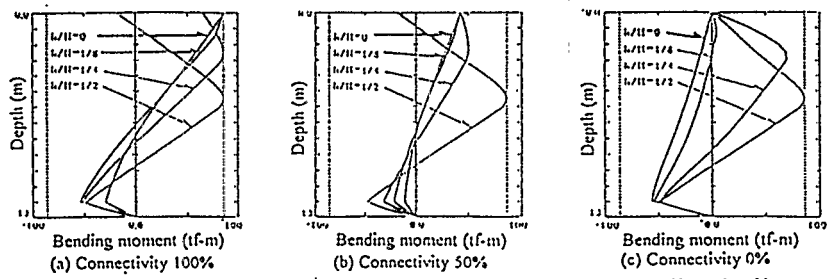

Figure 11 Bending moment distribution : Y joint spliced pile, 600mm dia. pile

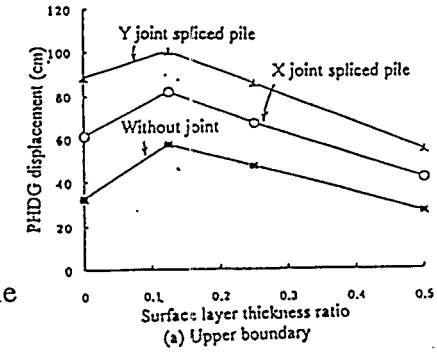

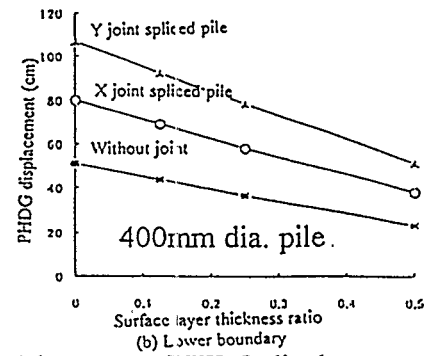

Figure 12 PHDG displacement Connectivity 100%

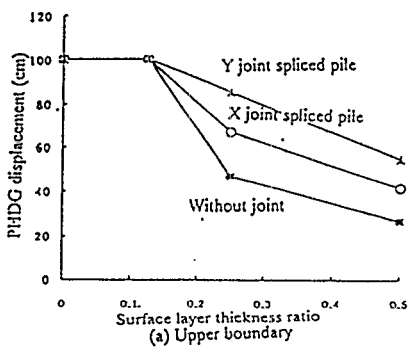

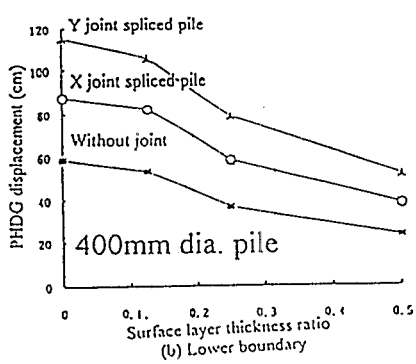

Figure 13 PHDG displacement Connectivity 0%

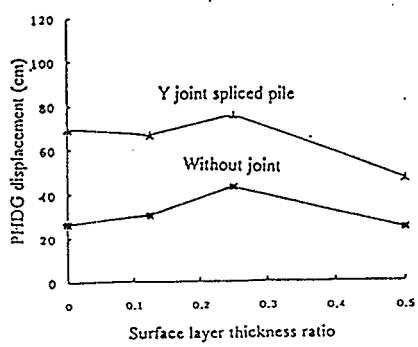

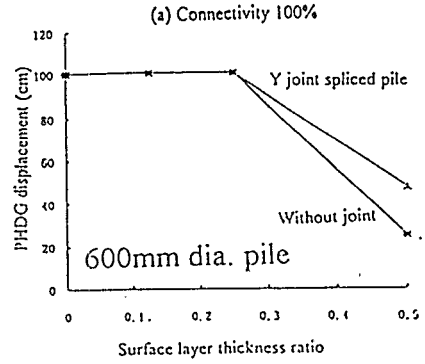

Figure 14 PHDG displacement Upper boundary

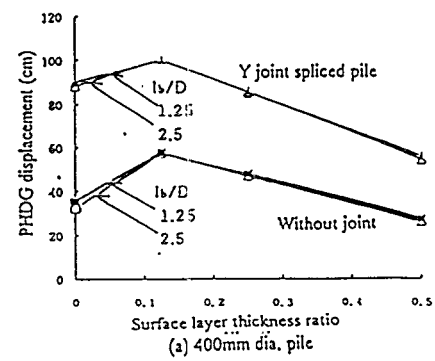

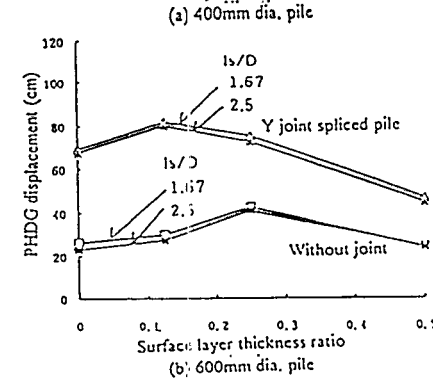

Figure 15 Affects of fixation ratio Upper boundary (l_b/D)

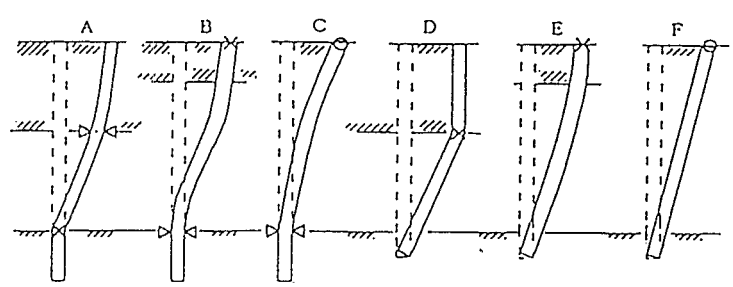

Figure 16 Patterns of ultimate situation